A minimalist bulk trade cumulus boundary layer model

SUNGSU PARK AND CHRISTOPHER BRETHERTON

Department of Atmospheric Science, University of Washington, Seattle

1. Introduction

It has long been recognized that shallow cumulus convection is an important process maintaining the characteristic temperature and moisture structure of the trades. Albrecht *et al.* (1979) explored the structure of the trades using their 2-layer bulk trade-cumulus model. However, the assumptions involved in their model are rather complex and caused some inconsistency, *e.g.*, the existence of virtual moisture source at the inversion as explored recently by Bellon and Stevens (2005). In this study, we construct a fully-consistent, minimal complexity bulk trade-cumulus boundary layer model that has similar dynamic assumptions to typical trade-cumulus parameterizations based on a single entraining-detraining cumulus updraft plume. Then, we will investigate some interesting issues of fundamental importance for understanding and parameterizing shallow cumulus cloud fields, especially over the ocean. Specifically, we aim at understanding

(1) the timescales for approach to a steady state,

(2) what regulates the equilibrium buoyancy and vertical velocity of shallow cumuli, which observations and LES models show to be much smaller than one predicted from adiabatic parcel ascent,

(3) how steady-state boundary layer structure depends on SST, mean subsidence rate, and *etc.*.

2. Model structure and key assumptions

Our model is Albrecht-like in structure but is discretized in a fully consistent way that does not suffer from the inconsistency between inversion heat and moisture flux that Albrecht's model experienced. The conservative thermodynamic variables we use are the liquid virtual potential temperature ($\theta_{vl} \equiv \theta_l \cdot (1 + \eta \cdot q_t)$, where θ_l is liquid potential temperature and $\eta = 0.61$) and total specific humidity ($q_t = q_v + q_l$). The convecting layer consists of a subcloud mixed layer (**ML**) and a cloud layer (**CL**) with linear gradients, topped by a sharp trade inversion (see Fig.1). Turbulent flux in CL is calculated from the mass flux parameterization ($\overline{\omega' a'} = g \cdot M_c \cdot (a_c - \bar{a})$), and vertical variations of cumulus mass flux (M_c where 'c' means cloud) and in-cloud conservative scalars (a_c) are uniquely determined by specifying a fixed fractional lateral entrainment (ε) and detrainment (δ) rate of a *single* updraft cumulus plume. The properties of conservative scalars at the CL base are set to be identical to those of the ML.

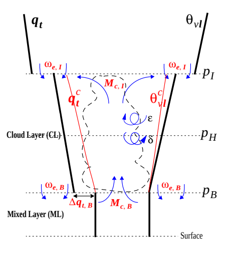

Figure 1. Structure of a minimal-complexity, bulk trade cumulus model.

Given a thermodynamic profile at current time step t and two guesses of the cumulus mass flux at CL base ($M_{c,B}$), we find tendencies for each $M_{c,B}$ of the key 5 prognostic variables - $\theta_{vl,M}$, $q_{t,M}$, $\theta_{vl,H}$, $q_{t,H}$, and p_I where subscripts M, H, and I stand for ML, midpoint of CL, and inversion base (see Fig.1). These are calculated by sequentially applying the balance equations of (1) ML heat budget assuming continuity of θ_{vl} across the ML top, (2) ML moisture budget assuming cloud base height (p_B) is tied at the lifting condensation level (LCL) of the ML air, (3) CL heat budget, (4) CL moisture budget, and (5) mass and heat balance constraints in the infinitesimally thin inversion layer. At time step $t + \Delta t$, we use the following flux consistency condition at the inversion base to constrain humidity jump across the ML top ($\Delta q_{t,B}$),

$$\frac{q^c_{t,I} - \overline{q_{t,I}}}{\Delta q_{t,I}} = \frac{\theta^c_{vl,I} - \overline{\theta_{vl,I}}}{\Delta\theta_{vl,I}}, \qquad (1)$$

which fully determines thermodynamic profile at $t + \Delta t$. Finally, the correct $M_{c,B}$ is calculated from the following entrainment closure at the inversion:

$$\omega_{e,I} = A \cdot g \cdot M_{c,I} \cdot \frac{(\theta^c_{v,I} - \overline{\theta_{v,I}})}{\Delta\overline{\theta_{vl,I}}}. \qquad (2)$$

Equation (2) is a simple way of relating the entrainment to the typical buoyancy of cumulus updrafts reaching the inversion base ($\tilde{\theta}_{v,I} \equiv \theta^c_{v,I} - \overline{\theta_{v,I}}$), the idea being that $\tilde{\theta}_{v,I}$ is roughly proportional to their typical 'overshoot' kinetic energy. By combining with Eq.(1), Eq.(2) at $t + \Delta t$ can also be written as

$$A \cdot (\theta^c_{v,I} - \overline{\theta_{v,I}}) + (\theta^c_{vl,I} - \overline{\theta_{vl,I}}) = 0. \qquad (2a)$$

For the BOMEX case, a reasonable value is A=5 based on Siebesma *et al.*'s (2003) conditionally sampled estimates from LES simulation.

3. Results - BOMEX Case Study

We applied our model to the BOMEX case, a steady state non-precipitating trade wind cumulus regime. We used fixed values of SST = 300.4 K, large scale divergence $D = 3 \cdot 10^{-6}$, surface exchange velocity $\omega_{t,s} = 0.1$ Pa s^{-1}, radiative cooling rate R = 2 K day^{-1}, $\varepsilon = 2 \cdot 10^{-6}$ Pa^{-1}, and $\delta = 2.7 \cdot 10^{-6}$ Pa^{-1}. After model reached to the steady state, we raised SST by 2K. A comparison with LES simulation was also performed.

(a) Transitional Behavior

Figure 2 shows the time evolution of several key variables. Within a few days, a steady state is achieved over the initial SST. When SST jumps, both $M_{c,B}$ and entrainment rate ($\omega_{e,B}$) at ML top increase abruptly. ML temperature increases rapidly in response to enhanced surface heat flux, while ML humidity decreases initially due to strong entrainment drying that more that compensates for enhanced surface moisture flux. Interestingly, LES simulation produced similar drying of ML humidity at the early stage of transition (not shown). Increased surface fluxes cause $M_{c,I}$ and $\omega_{e,I}$ at the inversion base to increase. The PBL deepens and the CL becomes warmer and drier. Comparison of the two steady states indicate increased gradients of the CL thermal and moisture profiles in association with CL deepening.

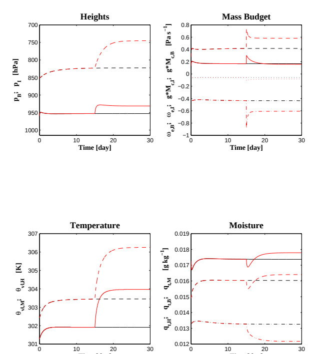

Figure 2. Model simulation of the BOMEX case. SST is raised by 2K at the end of day 15th.

Figure 2 also shows the differences of adjustment time scales between subcloud ML and CL properties. In general, there is rapid adjustment of the ML properties and cloud base height on a timescale less than a day, and a much slower adjustment of CL properties and trade inversion height on a divergence timescale of several days. Due to compensating entrainment drying, ML humidity adjusts more slowly than ML temperature.

Our treatment of cumulus mass flux and in-cloud properties as diagnostic variables implicitly assumes that the time scale of convective overturning process in the CL is negligibly small compared to the other thermodynamic time scales. In order to check if this is the case, we ran the LES for two days, with the SST jump at the end of simulation day 1. Figure 3a shows transitional behaviors of LES simulated $M_{c,I}$, updraft fractional area ($\sigma_{c,I}$) and vertical velocity ($w_{c,I}$) at the inversion base, estimated from conditionally-sampled cumulus core updrafts. $M_{c,I}$ responds almost instantaneously to the SST jump due to abrupt increase of $\sigma_{c,I}$. Soon thereafter, $M_{c,I}$ slowly adjusts to its new equilibrium value as in our bulk model. In contrast, $w_{c,I}$ does not show abrupt response, but gradually increases as the PBL deepens. Comparison of $M_{c,I}$ and $w_{c,I}$ clearly indicates that the time scale of convective overturning process in the CL is short compared to the other thermodynamic time scales.

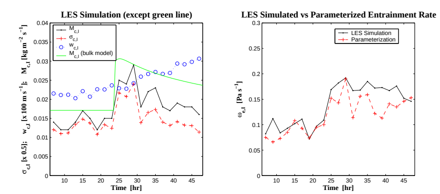

Figure 3. LES simulation with +2K SST jump at the end of 24th hr. (a) Cumulus mass flux ($M_{c,I}$), updraft fractional area ($\sigma_{c,I}$), and updraft vertical velocity ($w_{c,I}$) at the inversion base with bulk-model simulated $M_{c,I}$, (b) comparison of simulated and parameterized entrainment rates

An independent test of our entrainment parameterization [Eq.(2)] was performed using the LES simulation. After calculating individual terms on the R.H.S., $\omega_{e,I}$ were estimated using Eq.(2) and compared with $\omega_{e,I}$ estimated from the tendency of p_I. As shown in Figure 3b, our parameterization depicts the LES simulated entrainment rate reasonably well. Equation (2) slightly underestimates entrainment rate during the transitional period, but other estimation errors (*e.g.*, identification of inversion base and top) may contribute to this discrepancy.

(b) Cumulus 'Penetrative Entrainment - Buoyancy' Feedback

Figure 4 shows the insensitivity of the steady-state solution to large changes in the penetrative entrainment parameter A. As the entrainment efficiency increases, nearly the same entrainment rate is sustained by compensating decrease in cloud buoyancy. This small decrease of cloud buoyancy can be achieved by very slightly warmer $\overline{\theta_{vl}}$ and drier $\overline{q_t}$ associated with enhanced entrainment rate.

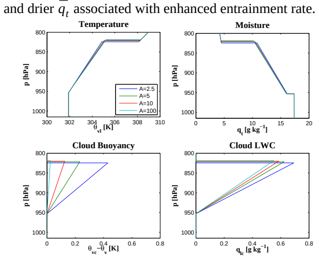

Figure 4. Vertical profiles of steady state solution for the BOMEX case (before SST jump) with various choices of the penetrative entrainment efficiency parameter, ***A***.

This illustrates a key feedback process that regulates the buoyancy and vertical velocity of cumulus clouds. If the sounding has enough conditional instability, cumuli develop that have vigorous updrafts when they reach the trade inversion layer. These entrain warm air which stabilizes the cumulus layer, reducing the buoyancy and vertical velocity of cumulus clouds at the trade inversion base until a balance is achieved between penetrative entrainment and mean subsidence at the trade inversion. The required cloud buoyancy for this balance is so small that the boundary layer thermodynamic profiles and the mean cloud liquid water content are similar to those found by assuming clouds have zero buoyancy (essentially the A=100 case).

(c) Steady state behavior

Figure 5 contours some interesting variables from steady state model solutions over a range of SST and divergence. The steady states span a wide variety of cloud layer depths. As expected, weak divergence and warm SST promote a deep trade inversion, thicker CL depth, and stronger $M_{c,B}$. The inversion-base relative humidity, RH_{inv} which can regulate the 'passive cloud cover' not associated with the small area coverage of active updrafts, tends to decrease as SST increases but is relatively insensitive to changes in large scale divergence.

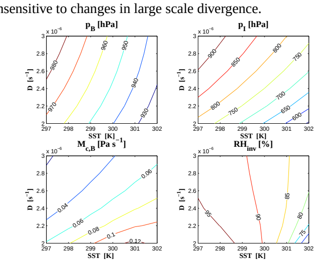

Figure 5. Approach to steady state for various SST and divergence.

4. Conclusion

We have constructed a fully-consistent, minimalist bulk trade-cumulus boundary layer model based on a single entraining-detraining cumulus updraft plume. Simulated steady state and transitional behaviors tested for the BOMEX case are reasonably similar to those simulated by LES. It was shown that the implicit model assumption that the time scale of convective overturning process is negligibly small compared to the other thermodynamic time scales is valid. Based on the simulation results, we argue that *the stabilization of temperature profile by cumulus penetrative entrainment is the key feedback process that keeps the equilibrium buoyancy of shallow cumuli to be very small.*

There are some obvious and important extensions we are currently trying to add, such as the inclusion of stratocumulus clouds and associated radiative-convective-entrainment feedback.

5. Acknowledgements

We are grateful to Peter Blossey for running the LES model and funding from the DOE Atmospheric Radiation Measurement Program.

6. References

Albrecht, B. *et al.*, 1979 : A model of the thermodynamic structure of the trade-wind boundary layer: Part I. Theoretical formulation and sensitivity tests. *J. Atmos. Sci*, **36**, 73-98.

Siebesma, A. *et al.*, 2003 : A large eddy simulation intercomparison study of shallow cumulus convection. *J. Atmos. Sci*, **60**, 1201-1219.

Bellon, G. and B. Stevens, 2005 : On bulk models of shallow cumulus convection. *J. Atmos. Sci*, in press.